

Green Synthesis Of Zno Nanoparticles Using Pomegranate Fruit Extract

Rana H. Adlan¹, Dr. Jalal Y. Mustafa², Dr. Orooba M.Faja³

¹Researcher, Basra University.

²Professor, Veterinary Public Health, College of Veterinary Medicine- University of Basra.

³Assistant professor, Veterinary Public Health, College of Veterinary Medicine- University of Al-Qdisiyah.

DOI: 10.47750/pnr.2022.13.S08.59

Abstract

Today, environmentally friendly solvent systems and eco-friendly reducing and capping agents have been used to create "Green" nanoparticles. The goal of the current work was to examine the manufacture of zinc oxid nanoparticles using pomegranate fruit extract as a reducing agent. In UV-vis spectra, the distinctive surface plasmon absorption peak of zinc at 370 nm served as proof that nanoscale zinc had formed. Scanning electron microscopy (SEM), energy dispersive X-ray analysis (EDAX), X-ray diffraction (XRD), and Fourier transform infrared (FTIR) spectroscopy were used to analyze the morphology and crystalline nature of the produced zinc molecule. Study the chemical composition of the peel extract by GC-MS chromatogram (Phytochemical analysis). Twenty-one significant peaks and the components matching to the peaks were found in the Punica granatum peel ethanolic extract used in the current study's chemical composition GC-MS chromatogram (Phytochemical) analysis. The current findings suggest that Punica granatum includes a number of bioactive ingredients.

Keywords : Pomegranate peel, extraction, , Bio-active compounds, Phytochemical analysis, GC-MS.; Biosynthesis ; and zinc oxide nanoparticle.

Introduction

The discipline of nanotechnology is expanding daily, having an impact on all aspects of human life, and inspiring an increasing amount of interest in the life sciences, particularly in the fields of biotechnology and biomedical devices (Singh et al. 2015; Prabhu et al. 2015). . Nanotechnology is exhibiting significant development in the food business and is anticipated to increase rapidly in the coming years, despite the fact that it is still relatively new compared to other fields of application. Nanotechnology is a multidisciplinary technology that can offer a wide range of novel applications (Rai et al., 2012).

Nanotechnology extends the increases different food items' shelf lives and lessens food waste as a result of microbial contamination (Pradhan et al., 2015).Using environmentally safe substances as reducing agents rather than possibly dangerous chemicals has made the green production of nanoparticle metals more advantageous than chemical synthesis. (Abdeen et al.,2014; Abd Ali, & Shareef (2021).

NPs can be grouped according to their origin and chemical composition. According to their origin, NPs are classified into three types: (1) natural, (2) incidental, and (3) manufactured NPs (Kendall and Holgate, 2012). According to their composition, NPs are classified into two types: organic (carbon-containing) and inorganic NPs (metal –containing).

Mechanisms Despite the fact that the precise mode of action for NPs' antibacterial capability against microbial infections is not fully understood, it has been observed that NPs can exert their antimicrobial impact either directly or by generating secondary active agents. Damage to the cell wall or plasma membrane, disruption of metabolic pathways, oxidation of cellular components, or DNA damage are the main factors that prevent microorganisms from growing (Kaur et al. 2011; Li et al. 2008). The size, shape, concentration, and interaction of NPs with the target pathogens all affect how they work as antimicrobials. According to studies, NPs' capacity to penetrate cell surfaces and, as a result, their antimicrobial activity, improves with decreasing size (Buzea et al. 2007; Padmavathy and Vijayaraghavan 2008; Bera et al. 2014).

Materials and methods

Preparations of aqueous pomegranate extract

The Preparation of aqueous pomegranate extracts was done using the method as described previously (Loo et al., 2012). Briefly, 1 kg of pomegranate was weighed, washed with distilled water, dried at room temperature, cut in small pieces, and grounded using blinder. Then, the pomegranate powder (10 gram) was weighed and mixed with 100 ml of distilled water at room temperature. The solution was heated to boiling point, maintained at that temperature for 5 minutes, and allowed to cool for 2 hours. The solution was then centrifuged at 4000 rpm to separate the liquid from the solid particles. The liquid was then further filtered using mesh fabrics to remove any remaining particles, yielding pure liquid extracts, The extracts thus prepared were used immediately

Synthesis of zinc nanoparticles

6.58 g of zinc nitrate was dissolved in 300 mL of double-distilled water to create the 0.1 M zinc nitrate hexahydrate solution ($Zn(NO_3)_2 \cdot 6H_2O$). To achieve complex formation, ten milliliters of the aqueous pomegranate extracts were gradually added dropwise into the solution while being stirred magnetically at 60 °C for around two hours. After stirring, the complex was collected and kept in a dark area for 72 hours.. observation of the 72-hour color transition from reddish brown to dark brown.then centrifuged at 10,000 rpm for 10 min and the pellets were collected. The separated pellets were kept in airtight vials for future research after being dried in an oven at 80 C for 8 hours. As opposed to (Umar et al., 2018). I noticed the hue going from brown to dark brown.

3.4.5 Biosynthesized ZnONPs' Characterization

Utilizing a variety of instrumental approaches, the following characteristics of the produced zinc oxide nanoparticles (ZnNPs) of aqueous pomegranate abstract were confirmed:

A. Scanning Electron Microscopy (SEM)

The form and size of the biosynthesised zinc oxid nanoparticles (ZnONPs) in the aqueous pomegranate abstracts were determined using scanning electron microscopy.. An aluminum-coated copper grid and films on the SEM apparatus were each given one drop of a solution containing zinc oxide nanoparticles before waiting for five minutes. The surplus solution was then taken off the grid by using blotting paper and drying it. Readings were taken at constant voltage at magnifications of 5000, 10000, 20000, and 50000, and the succeeding nanoparticles' size appropriation was assessed using SEM micrographs (Khoshnamvand et al., 2019). This test was carried out at the Science and Technology Ministry, as were all biogenic ZnO NP characterizations.

B. X-Ray Diffraction Analysis (XRD)

The manufacture and scale of ZnONPs were characterized using the X-ray diffraction analysis, including their size and crystallinity. After positioning the sample on a glass slide and determining the angle of the Bragg at 2 °, the XRD measurements were carried out. Centrifugation of the biogenic ZnONPs solution was done for 30 minutes at 10,000

rpm. The pellet was rinsed three times with 20 milliliters of deionized water. X per Rota Flex Diffraction Meter, Cu K radiation, = 1,5406 Å, 40.0 kV voltage, 30.0 mA x ray current, continuous scan, range (10,000-90,000 deg), speed approximately 0.2000 deg / min in 1.20 sec., dried mixture of biogenic ZnONPs, and XRD patterns were captured (Ojha et al., 2017). The Debye-Scherrer equation was used to determine the crystallite size for ZnONPs (Sankar et al., 2013; Alwan & Al-Saeed 2021).

$$D = K\lambda / \beta \cos \theta$$

Where; D = diameter of NPs dimension, K = a constant (0.94 is used along with cubic symmetry to harmonize spherical crystallites), B = Full Width at Half Maximum (FWHM) and θ (Bragg angle) = the angle of diffraction.

C. UV-VIS Spectrophotometer Analysis

In order to investigate the optical characteristics and stability of nanoparticles, the UV-visible spectroscopy absorption is essential. After diluting the small aliquot sample in distilled water to determine its concentration, the UV-visible reduction media spectrum was evaluated to determine the bio-reduction of the biogenic ZnONPs. The surface Plasmon resonance was measured with a UV-Visible Spectrophotometer (SPR) . between the wavelengths of 200 and 800 nm. The surface Plasmon particle resonance nanoscale peak characteristics can be seen in the UV-Visible absorption spectrum (Gauthami et al., 2015).

D. Fourier Transforms Infrared (FTIR) Spectroscopy Analysis

FTIR spectroscopy was used to examine the manufactured zinc nanoparticles (ZnONPs) of pomegranate methanol bark extract (dry pellet). to categorize the samples' functional categories using the peak positions at wavelengths between 400 and 4000 cm^{-1} . Centrifuging the biogenic ZnONPs solution at 10000 rpm/30 min was done for the FTIR calculations (Tugarova et al., 2018). 20 ml of deionized water was used to wash the pellet three times. After drying, they were used to look at the biogenic ZnONPs.

Gas Chromatography Mass Spectrum Analysis (GC-MS)

A phytochemical analysis of *Punica granatum* (pomegranate) peel extract was performed using GC-MS, according to Pongpuntaruk (2010), Hameed et al. (2015), and Al-Tameme et al. (2015b). There have been numerous phytoconstituent analyses performed globally using GC-MS technology (Priya et al., 2011). Using Shimadzu GC-2010 gas chromatography combined with QP2010 mass spectrometer, the components of methanolic extract of pomegranate juice (Salami variety) were identified. A 30 m glass capillary column with a film thickness of 0.25 μm was used to inject the material into the GC-MS. Using a constant flow rate of 1 ml/min, helium was used as the carrier gas. Temperatures in the injector and detector were maintained at 250 °C. The temperature range for the GC was 60°C to 280°C at 15°C per minute. 1:30 split ratio The length of the GC as a whole is 35 minutes. At 70 eV, An MS was documented. The MS scan settings were a detector voltage of 1.0 kV, a mass range of m/z 40–1000, a scan interval of 0.5 s, and a scan speed of 1000 amu s⁻¹. Utilizing the NIST08, WILEY8, and FAME Libraries databases, chemicals were identified. A comparison was made between the mass spectra of the particular unknown chemical and the known compounds kept in the software database Libraries. The components of the test materials' names, molecular weights, and structures were determined.

4. Results

Preparation and Characterization of ZnO nanoparticles

Visual Observation or Colour Modification of Biosynthesized ZnONPs.

The initial step in improving the manufacture (or creation) of biogenic ZnONPs using aqueous pomegranate extract is to alter (or change) the color of the particles (ZnONPs). As a result, the current study's investigation reveals that when pomegranate abstract was gradually added to the colorless zinc nitrate solution, the color changed from brown

to dark brown after 72 hours and remained there (Figure 2). This finding suggests that it was successful to fabricate or synthesize biogenic zinc oxide nanoparticles using aqueous pomegranate extract.

Biosynthesis(green synthesis) and characterization of ZnONPs

The environmentally friendly synthesis of zinc oxide nanoparticles was intended to create ZnONPs from aqueous pomegranate extract. In the present work, biosynthesized ZnONPs were assessed according to certain standards or criteria related to their properties, including color modification, SEM, XRD, and UV-VIS spectroscopy

Scanning Electron Microscopy (SEM)

The Scanning Electron Microscope (FE-SEM) is an effective technique for investigating the morphology of a material and offers useful details on nanoparticle size and shape. Figures (1) of ZnO NPs produced with pomegranate extract High-roughness agglomerated nanoparticles that are semi-spherical can be seen. The surface morphology of nanoparticles confirms their agglomerated shape. The SEM picture of the nanoparticles shows that they are approximately 38.30 nm in size on average. 34.27 nm and 38.30 nm).

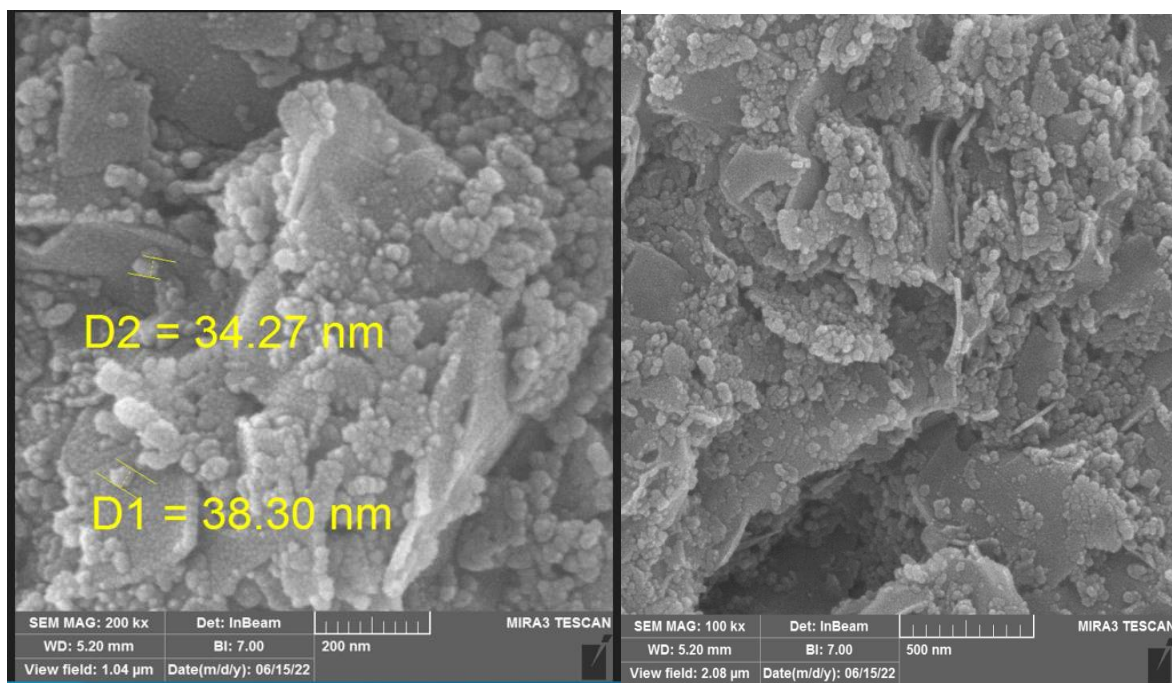


Figure 1: Scanning Electron Microscopy (SEM) Shows the Morphology and Size of Biogenic Nanoparticles (ZnONPs), different magnifications 200nm and 500 μm .

X-Ray Diffraction (XRD) Analysis

The results of the present investigation offer solid justification for the production of biogenic nanoparticles utilizing XRD analysis. (Figure 2), showed The strong and narrow diffraction peaks indicate that the product has good crystalline structure. the results of XRD exhibited four blatant diffraction peaks. at 2θ values, 12.62, 15.013, 16.249, 19.677, 21.262, 22.177, 23.596, 24.803, 28.091, 31.243, 34.056, 35.856, 39.568, 41.352, 42.409, 47.202, 56.243, 59.373, 62.555, 66.08, 67.647, 68.717, 73.984 and 76.806 for ZnONPs .

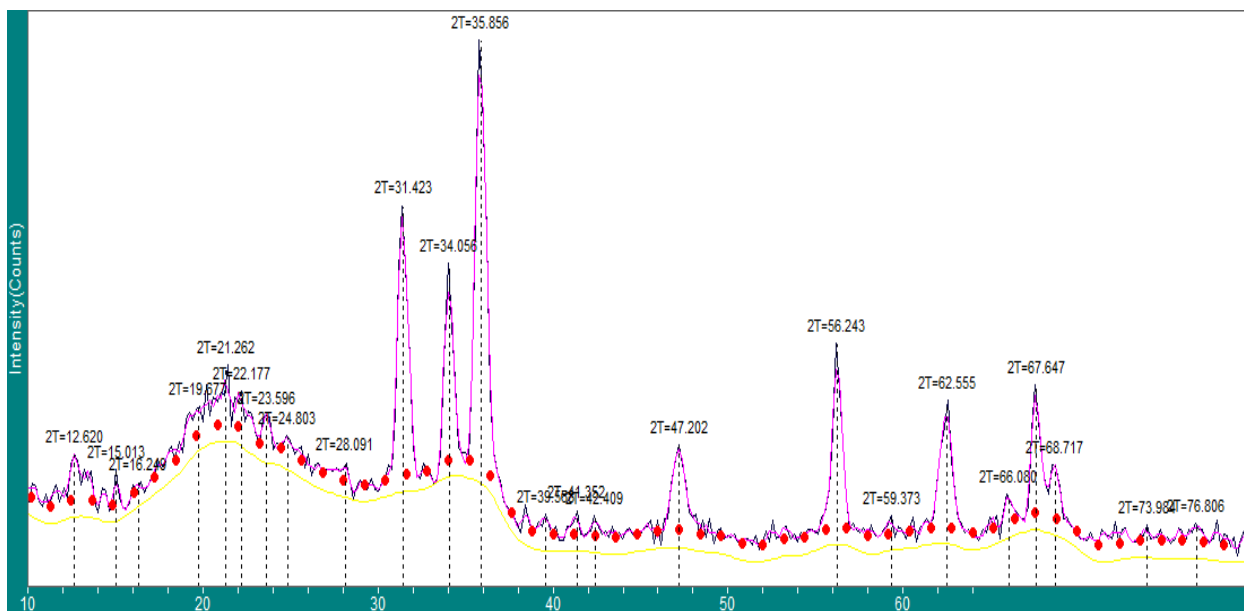
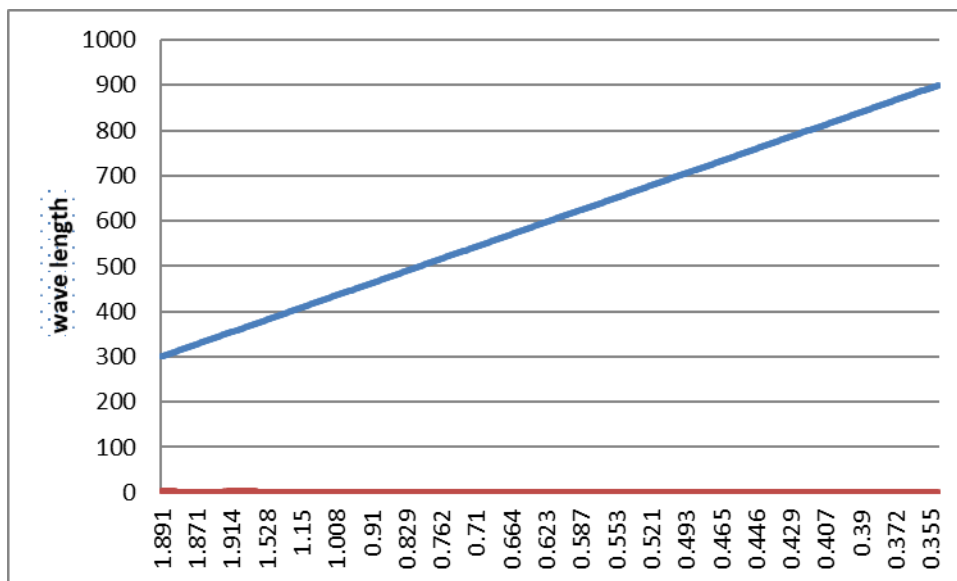


Figure 2: X-ray Diffraction Pattern of Biogenic Nanoparticles (ZnONPs).

Ultraviolet-Visible (UV-VIS) Spectroscopy

ZnO NPs' existence was verified by a substantial absorption band with a maximum of 370 nm in the 320–400 nm range. The absorption peak at 370 nm Figure (3) .



UV-Absorption

Figure 3: UV-Vis After 72 hours of incubation, the spectrum of biotic silver nanoparticles was seen.

Fourier Transform Infrared (FT-IR) Spectroscopy

The composition and synthesis of functional groups in synthesized ZnO are revealed by FT-IR. The spectrums of the samples were identified utilizing at a wavelength range of 4000–400 cm⁻¹, as shown in Figure (4) . Peaks are observed

in 3345.89, 2925.48, 1625.7, 1401.03, 1076.08, 558.291, 451.261, and 429.084 cm^{-1} . The peak at (3345.89) cm^{-1} corresponds to N-H(Amine) bond vibration of amine or amide groups. The lower wavenumber absorption peaks (429.084) cm^{-1} and the peak at 2925.48 cm^{-1} are attributed to the C=O stretch, which identifies the chemical as a ketones. the peak at (1625.48) cm^{-1} corresponding to (C-N) stretching vibrations of aromatic amines. Peak 1401.03 cm^{-1} correspond to (C-H) bending in alkanes. the peak at (1076.08) cm^{-1} and (558.291) cm^{-1} confirm C-X stretching in alkyl halides. Finally, the band at (451.261 cm^{-1}) and (429.084 cm^{-1}) were due to C-N-C bending in amines. In order to produce ZnO, which was seen as bands and an efficient capping agent, the biomolecules in the plant extract are in charge of reducing zinc ions. This aids in the production of NPs. These findings collectively indicated the presence of functional groups in the biosynthesized ZnONPs, which is important for their functionalities and applications.

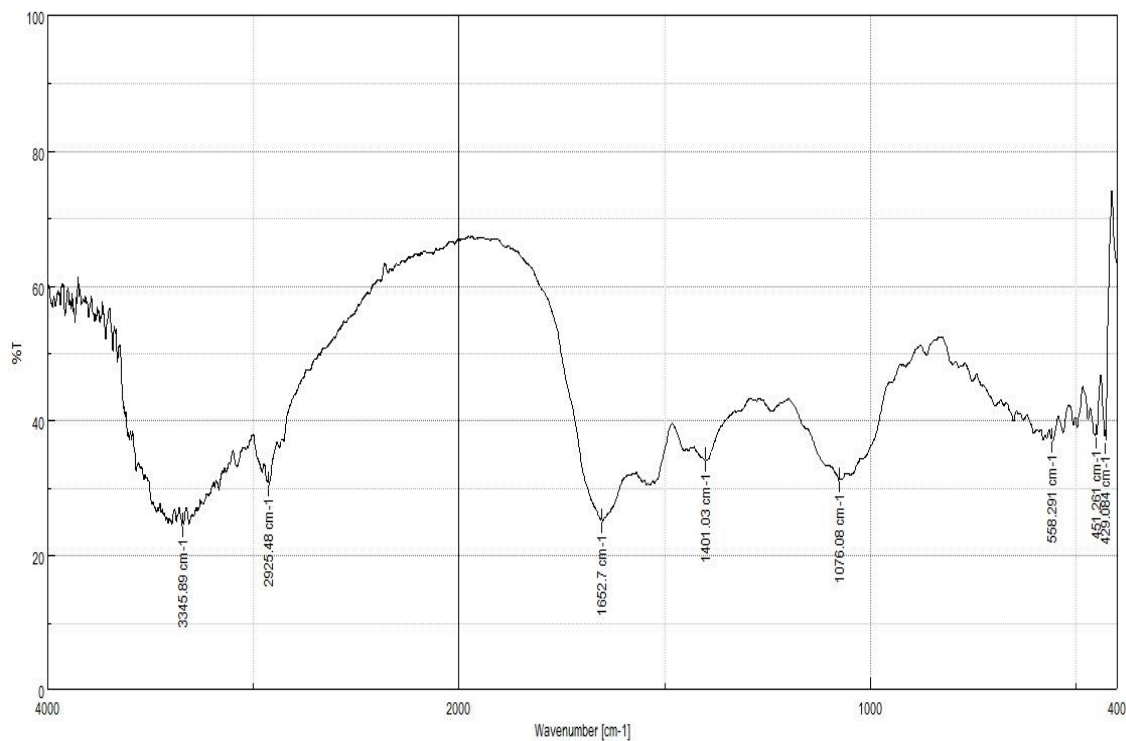


Figure (4): ZnO-NPs' FTIR spectrum demonstrates that they were successfully made using green synthesis.

GC-MS Analysis of pomegranate Ethyl Acetate Extract

Recent studies have used GC-MS to identify the different components in ethanolic pomegranate extract based on peak regions, molecular weight, and molecular formula. The relationship between the peak regions and the amount of the compound in the active band has been established. Based on peak area percentage, retention time, molecular formula, and molecular weight, GC-MS analysis was utilized in this investigation to identify 21 chemicals. (Table 1, Fig. 5). The major constituents were 2,4-Dihydroxy-2,5-dimethyl-3(2H)-furan-3-one (9.459), 2-Thiazolamine, 4,5-dihydro (15.235), 4-Pyrimidinol, 5-methoxy (20.013), 4H-Pyran-4-one, 2,3-dihydro-3,5-dihydroxy-6-methyl (21.271), 2,3-Dihydrooxazole, 2-t-butyl-3-pivaloyl (22.889), Cyclohexane, 1,4-diethoxy-, trans- (23.227) Hexadecaneperoxoic acid, 1,1-dimethyl-3-[(1-oxohexadecyl)oxy]propyl ester (27.145), Hexanedioic acid, dioctyl ester (31.079), 3-Pentanamine, N,N'-1,2-ethanediyliidenebis[2,4-dimethyl (33.442), Octadecanoic acid (34.883), Hexadecanoic acid, 2-hydroxy-1-(hydroxymethyl)ethyl ester (41.629), 9-Octadecenoic acid (Z)-, 2,3-dihydroxypropyl ester (43.371), Cyclopropylpyrrol-4-[3-(1H-imidazol-4-yl)propoxy] phenylmorphomethanone oxime (49.735), Ethanamine, N-ethyl-N-nitroso (48.215), Pyrimidine, 4-chloro-5-ethoxy-2-methyl- (51.742), Pyrogallol (52.588), 4H-Pyran-4-one, 3,5-dihydroxy-2-methyl- (55.957), 3,7,11,15-Tetramethyl-2-hexadecen-1-ol (60.280), Gallic acid (60.615), Punicalin (61.203), D-Allose (61.500).

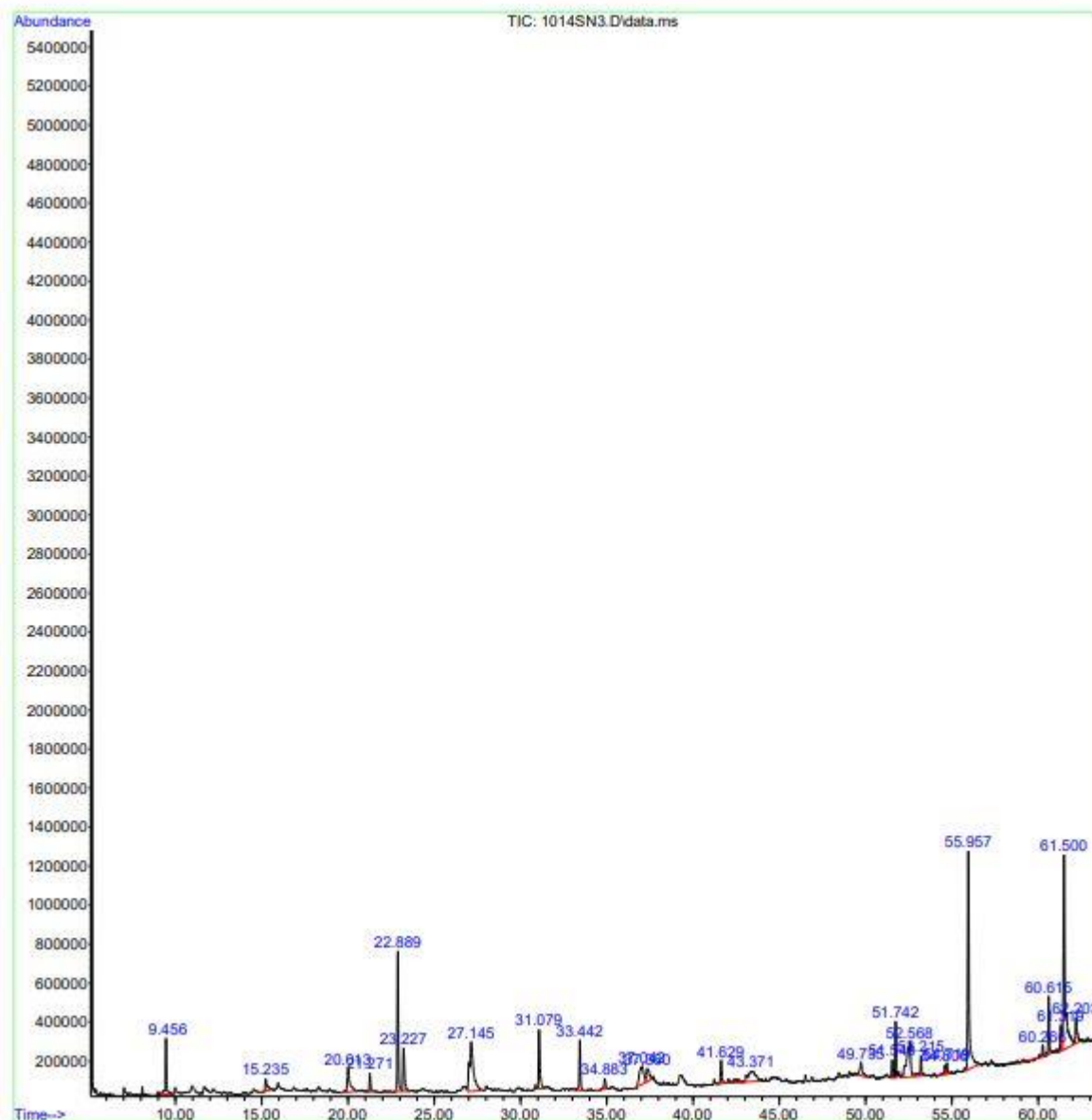


Figure 5: GC-MS Chromatogram of ethanolic extract of the Punica granatum peel

Table(1) Punica granatum Juice ethanolic extracts were used to identify phytochemicals using GC-MS.

Peak	R.Time	Component Name	Area	Molecular Formula	Molecular weight
1	9.456	2,4-Dihydroxy-2,5-dimethyl-3(2H)-furan-3-one	0.73	C ₅ H ₆ O ₅	146
2	15.235	2-Thiazolamine, 4,5-dihydro-	0.44	C ₆ H ₁₂ O ₃	132
3	20.013	4-Pyrimidinol, 5-methoxy-	0.16	C ₅ H ₆ N ₂ O ₂	126

4	21.271	4H-Pyran-4-one, 2,3-dihydro-3,5-dihydroxy-6-methyl	6.07	C6H8O4	144
5	22.889	2,3-Dihydrooxazole, 2-t-butyl-3-pivaloyl-	0.25	C12H21NO2	211
6	23.227	Cyclohexane, 1,4-diethoxy-, trans-	0.49	C10H20O2	172
7	27.145	Hexadecaneperoxoic acid, 1,1-dimethyl-3-[(1-oxohexadecyl)oxy]propyl ester	1.24	C37H12O5	596
8	31.079	Hexanedioic acid, dioctyl ester	0.63	C22H42O4	370
9	33.442	3-Pentanamine, N,N'-1,2-ethanediyldenebis[2,4-dimethyl	1.28	C16H32N2	252
10	34.883	Octadecanoic acid	0.5	C18H36O2	84
11	41.629	Hexadecanoic acid, 2-hydroxy-1-(hydroxymethyl)ethyl ester	0.48	C19H38O4	330
12	43.371	9-Octadecenoic acid (Z)-, 2,3-dihydroxypropyl ester	0.89	C21H40O4	356
13	49.735	Cyclopropylpyrrol4-[3-(1H-imidazol-4-yl)propoxy] phenylmorphomethanone oxime	0.43	C16H19N3O2	177
14	48.215	Ethanamine, N-ethyl-N-nitroso	0.18	C4H10N2O	102
15	51.742	Pyrimidine, 4-chloro-5-ethoxy-2-methyl-	0.44	C7H9ClN2O	172
16	52.588	Pyrogallol	2.25	C6H6O3	126
17	55.957	4H-Pyran-4-one, 3,5-dihydroxy-2-methyl-	0.32	C6H6O4	142
18	60.280	3,7,11,15-Tetramethyl-2-hexadecen-1-ol	0.31	C20H40O	296
19	60.615	Gallic acid	43.25	C6H6O3	126
20	61.203	Punicalin -	1.05	C16H34B2O8	376
21	61.500	D-Allose	3.56	C6H12O6	180

Discussion

Biosynthesis characterization of ZnONPs.

Recently, the green manufacturing of zinc oxide nanoparticles (ZnONPs) using plant extracts has become increasingly popular. Metal ions and biological systems have been demonstrated to interact, reducing them into metallic nanoparticles (Beveridge and Murray, 1980 ; Beveridge, et al., 1997). The utilization of these NPs produced through biosynthesis in various medical applications has been noted in numerous research (Kumar et al., 2013; Jasim et al.,

2020).. The current study looks into a successful strategy, a successful technique, for producing ZnONPs using aqueous pomegranate extract as a starting material. The green synthesis utilized the bioactive component from the pomegranate extract. in the current work and served considered to be an essential step in the formation of NPs, as a reducing metal ion and capping agent (Javed et al., 2020). Parveen and Rao (2015) found in their research that the increased color intensity of incubated NPs was a need for the initial step in the manufacturing of NPs. In the current investigation, the presence of the bioactive secondary metabolites of pomegranate extract showed the synthesis of biogenic zinc nanoparticles by the change in color and the persistent hue (darkness). The appearance of this color or The excitation of surface plasmon vibration is what causes these color changes. in ZnONPs (Kumararaja et al., 2019). SEM analysis was used to describe the morphology and size of the biogenic zinc oxide nanoparticles (ZnO NPS) (SEM) Numerous papers have discussed the relationship between surface form and ZnO's synergistic activity (Fardood et al., 2017) The size of metallic nanoparticles affects their characteristics and function.. Figure (1). In this instance, our conclusions regarding the size and form of NPS were congruent and comparable to those of others (Gauthami et al., 2015). Nanoparticle surfaces contain cellular components that serve as capping agents and encourage aggregation. (Bélteky et al., 2019). The crystalline nature of the biosynthesized zinc oxide nanoparticles ZnONPs, which are produced as a result of the reduction of metal ions (Zn^{2+}) by the bioactive chemicals included in the plant extract, is depicted by the XRD pattern (Figure 2).. Additionally, Alsamhary (2020) reported the current large size of the biosynthesized nanoparticles. The presented XRD patterns are in agreement with previous reports on microstructures (Ghodake et al. 2010). he crystallites are nanoscale and have a high crystallinity, according to the sharp peaks. Scherrer's equation was used to estimate the average crystallite size of the produced ZnO nanoparticles (Shashanka et al., 2020). It was reported that a similar X-ray diffraction pattern observed (Chenn et al., 2011)and(Peng et al., 2012).

The Debye-Scherrer equation revealed that the average crystallite size of biosynthesized zinc nanoparticles was 38.30 nm (ZnONPs). This research supports the conclusions made public by Sathishkumar et al (2009) .

. Overall, the results of the present investigation and the aqueous pomegranate extract green synthesis according to the aforementioned key features are regarded as a good approach for manufacturing stable ZnONPs quickly.. Figure illustrates the visible peak in the UV-Vis spectrum at 370 nm after 72 hours of incubation as shown in Figure (3). The spectrum reveals the typical band-gap absorption of ZnO; this band is also related to the valence excitation of ZnO nanoparticles (nanocrystalline/nanosphere). The FT-IR data (Figure 4) demonstrated that the NPs of the pomegranate extract contained a variety of functional groups. Phenols, alcohols, alkanes, alkynes, and aldehydes were the compounds with these functional groups. Salim and his team reported comparable findings in 2017.. A number of processes, including electrostatic stability, steric stabilization, hydration force, and stabilization, appear to be used by the capping agents to stabilize NPs. (Kalpana, and Rajeswari., 2018).

GC-MS Analysis of pomegranate Ethyl Acetate Extract

Previous studies have shown that the plant portion and maturity stage have an impact on the variety and distribution of chemicals in pomegranates. According to (Wannes et al., 2010) In addition to the experimental design, environmental factors, genetic effects, ontogeny, variety, and plant components were all taken into consideration. (Vedashree et al., 2020). Pomegranate (*Punica granatum L.*) fruit contains abundant bioactive polyphenolic compounds (Lansky and Newman 2007). Pomegranate (*Punica granatum L.*) belongs to the Punicaceae family (Facciola et al., 1990 ; Alfeikaik, & AL-Hilfi., 2016).

Table (1) shows the results of qualitative phytochemical screening of 70% ethanolic extract of Pomegranate peels. contain metabolomes, retention times (RT), percentages, and the area under the peak molecular formula. The discovered chemicals' GC-MS chromatogram peaks are displayed in (Figure 5). These metabolomes were recognized as being associated with various chemical categories. The identity of the compounds present in the sample extracts is in agreement with previous works (Ulrike et al., 2011; Beatriz et al., 2018)

Conclusions

1- ZnO NPs are a good contender among other metal oxides because of their noble qualities and appealing traits that significantly toxicate organisms.

2-“ Due to the growth of eco-friendly technologies in materials science, "green" production of metallic nanoparticles has drawn more attention.

3- The current work illustrated the use of pomegranate fruit extract in the bioreductive production of nano-sized zno particles.

Numerous research suggest that ZnONPs could be produced utilizing a green synthesis method that includes a range of plants, fungi, bacteria, and algae. Furthermore, the research mentioned here show that these substrates, regardless of their source, serve as reducing and stabilizers or as chelating compounds..

References

1. **Pradhan, N.; Singh, S.; Ojha, N.; Srivastava, A.; Barla, A., Rai, V., et al. (2015).** Facets of nanotechnology as seen in food processing, packaging, and preservation industry. *BioMed Res. Int.* 2015:365672. doi: 10.1155/2015/365672
2. Kendall, M., & Holgate, S. (2012). Health impact and toxicological effects of nanomaterials in the lung. *Respirology*, 17(5), 743-758.
3. Prabhu, R. H., Patravale, V. B., & Joshi, M. D. (2015). Polymeric nanoparticles for targeted treatment in oncology: current insights. *International journal of nanomedicine*, 10, 1001.
4. Rai, M. K., Deshmukh, S. D., Ingle, A. P., & Gade, A. K. (2012). Silver nanoparticles: the powerful nanoweapon against multidrug-resistant bacteria. *Journal of applied microbiology*, 112(5), 841-852.
5. Singh, O. V. (Ed.). (2015). *Bio-nanoparticles: biosynthesis and sustainable biotechnological implications*. John Wiley & Sons.
6. Kaur, P.; Thakur, R.; Kumar, S.; Dilbaghi, N. (2011). Interaction of ZnO nanoparticles with food borne pathogens *Escherichia coli* DH5 α and *Staphylococcus aureus* 5021 & their bactericidal efficacy. *AIP Conf Proc* 1393:153–1
7. Li, X., & Heyer, W. D. (2008). Homologous recombination in DNA repair and DNA damage tolerance. *Cell research*, 18(1), 99-113.
8. Buzea, C.; Pacheco, I.I.; Robbie, K. (2007) .Nanomaterials and nanoparticles: sources and toxicity. *Biointerphases* 2:MR17–MR71s
9. Padmavathy, N.; Vijayaraghavan, R. (2008) .Enhanced bioactivity of ZnO nanoparticles-an antimicrobial study. *Sci Technol Adv Mater* 9:1–7
10. Bera, R.K; Mandal, S.M; Raj, C.R. (2014). Antimicrobial activity of luorescent Ag nanoparticles. *Lett Appl Microbiol* 58:520–526
11. Sirelkhatim, A.; Mahmud, S.; Seeni, A.; Kaus, N.H.M.; Ann, L.C.; Bakhori, S.K.M., Hasan, H., Mohamad, D. (2015). Review on zinc oxide nanoparticles: antibacterial activity and toxicity mechanism. *Nano-Micro. Lett.* 7, 1–24.
12. Vigneshwaran, N.; Bharimalla, A.K.; Prasad, V.; Kathe, A.A.; Balasubramanya, R.H.(2008). Functional behaviour of polyethylene-ZnO nanocomposites. *J. Nanosci. Nanotechnol.* 8, 4121–4126.
13. Ambika, S., & Sundrarajan, M. (2015). Green biosynthesis of ZnO nanoparticles using *Vitex negundo* L. extract: Spectroscopic investigation of interaction between ZnO nanoparticles and human serum albumin. *Journal of Photochemistry and Photobiology B: Biology*, 149, 143-148.
14. Loo, Colleen K., et al. (2012). "Transcranial direct current stimulation for depression: 3-week, randomised, sham-controlled trial." *The British Journal of Psychiatry* 200.1: 52-59.
15. Khoshnamvand, M.; Huo, C. and Liu, J. (2019). Silver nanoparticles synthesized using *Allium ampeloprasum* L. leaf extract: Characterization and performance in catalytic reduction of 4-nitrophenol and antioxidant activity
16. **Ojha, S.; Sett, A. and Bora, U. (2017).** Green synthesis of silver nanoparticles by *Ricinus communis* var. *carmencita* leaf extract and its antibacterial study. *Advances in Natural Sciences: Nanoscience and Nanotechnology*. 8(3), 35009. <https://doi.org/10.1088/2043-6254/aa724b>
17. **Gauthami, M.; Srinivasan, N.; Goud, N.; Boopalan, K. and Thirumurugan, K. (2015).** Synthesis of Silver Nanoparticles using *Cinnamomum zeylanicum* Bark Extract and its Antioxidant Activity. *Nanoscience & Nanotechnology-Asia*. 5(1), 2–7. <https://doi.org/10.2174/221068120501150728103209>
18. **Tugarova, A. V.; Mamchenkova, P. V.; Dyatlova, Y.A. and Kamnev, A.A., (2018).** FTIR and Raman spectroscopic studies of selenium nanoparticles synthesised by the bacterium *Azospirillum thioophilum*. *Spectrochim. Spectrochimica Acta - Part A: Molecular and Biomolecular Spectroscopy*. 192(1), 458–463. <https://doi.org/10.1016/j.saa.2017.11.050>
19. **Umar, H.; Kavaz, D.; Rizaner, N.(2018).** Biosynthesis of zinc oxide nanoparticles using *Albizia lebbeck* stem bark, and evaluation of its antimicrobial, antioxidant, and cytotoxic activities on human breast cancer cell lines. *Int. J. Nanomed.*, 14, 87–100. [CrossRef] [PubMed]

20. Hameed, I. H., Hussein, H. J., Kareem, M. A., & Hamad, N. S. (2015). Identification of five newly described bioactive chemical compounds in methanolic extract of *Mentha viridis* by using gas chromatography-mass spectrometry (GC-MS). *Journal of Pharmacognosy and Phytotherapy*, 7(7), 107-125.
21. Al-Tameme, H. J. M. (2015). Chemical profiles as chemotaxonomic tools for some species in Fabaceae in Iraq. *Al-Qadisiyah Journal of Pure Science*, 20(1), 88-99.
22. **Priya, D.; Rajaram ,K.; Suresh, K.P.(2011)**. Phytochemical studies and GC-MS analysis of *Caralluma fimbriata* Wall. *Int. J. Pharm. Res. Dev.*, 3(10): 105-110.
23. **Beveridge, T. J. & Murray, R. G. (1980)**. Sites of metal deposition in the cell wall of *Bacillus subtilis*. *Journal of bacteriology*, 141(2), 876-887.
24. **Beveridge, T. J.; Hughes, M. N.; Lee, H.; Leung, K. T.; Poole, R. K.;Savvaidis, I., & Trevors, J. T. (1996)**. Metal-microbe interactions: contemporary approaches. *Advances in microbial physiology*, 38, 177-243.
25. **Kumar, P.; Govindaraju, M.; Senthamilselvi, S. and Premkumar, K. (2013)**. Photocatalytic degradation of methyl orange dye using silver (Ag) nanoparticles synthesized from *Ulva lactuca*. *Colloids Surfaces B. Biointerfaces*. 103(1), 658–661. <https://doi.org/10.1016/j.colsurfb.2012.11.022>
26. **Jasim, N.A.; Al-Gasha'a, F.A.; Al-Marjani, M.F.; Al-Rahal, A.H.; Abid, H.A.; Al-Kadhmi, N.A.; Jakaria, M. and Rheima, A.M. (2020)**. ZnO nanoparticles inhibit growth and biofilm formation of vancomycin-resistant *S. aureus* (VRSA). *Biocatalysis and Agricultural Biotechnology*. 29(1), 101745. <https://doi.org/10.1016/j.cbab.2020.101745>
27. **Javed, R.; Zia, M.; Naz, S.; Aisida, S.O.; Ul Ain, N. and Ao, Q. (2020)**. Role of capping agents in the application of nanoparticles in biomedicine and environmental remediation: recent trends and future prospects. *Journal of Nanobiotechnology*.18(1), 172. <https://doi.org/10.1186/s12951-020-00704-4>
28. **Parveen, A. and Rao, S. (2015)**. Mechanistic approach of functionalized noble metal nanoparticles synthesis from *Cassia auriculata* L. *Journal Cluster Science*. 26(1), 1295–1303. <https://doi.org/10.1007/s10876-014-0813-2>
29. Taghavi Fardood, S., Ramazani, A., Moradi, S., & Azimzadeh Asiabi, P. (2017). Green synthesis of zinc oxide nanoparticles using arabic gum and photocatalytic degradation of direct blue 129 dye under visible light. *Journal of Materials Science: Materials in Electronics*, 28(18), 13596-13601.
30. Cheng, F., Shen, J., Peng, B., Pan, Y., Tao, Z., & Chen, J. (2011). Rapid room-temperature synthesis of nanocrystalline spinels as oxygen reduction and evolution electrocatalysts. *Nature chemistry*, 3(1), 79-84.
31. Peng, S., Okasinski, J. S., Almer, J. D., Ren, Y., Wang, L., Yang, W., & Sun, Y. (2012). Real-time probing of the synthesis of colloidal silver nanocubes with time-resolved high-energy synchrotron x-ray diffraction. *The Journal of Physical Chemistry C*, 116(21), 11842-11847.
32. Shashanka, R., Esgin, H., Yilmaz, V. M., & Caglar, Y. (2020). Fabrication and characterization of green synthesized ZnO nanoparticle based dye-sensitized solar cells. *Journal of Science: Advanced Materials and Devices*, 5(2), 185-191.
33. **Gauthami, M.; Srinivasan, N.; Goud, N.; Boopalan, K. and Thirumurugan, K. (2015)**. Synthesis of Silver Nanoparticles using *Cinnamomum zeylanicum* Bark Extract and its Antioxidant Activity. *Nanoscience & Nanotechnology-Asia*. 5(1), 2–7. <https://doi.org/10.2174/221068120501150728103209>
34. **Béteky, P.; Rónavári, A.; Igaz, N.; Szerencsés, B.; Tóth, I.Y.; Pfeiffer, I.; Kiricsi, M. and Kónya, Z. (2019)**. Silver nanoparticles: Aggregation behavior in biorelevant conditions and its impact on biological activity. *International Journal of Nanomedicine*. 14(1), 667–687. <https://doi.org/10.2147/IJN.S185965>
35. **Alsamhary, K.I. (2020)**. Eco-friendly synthesis of silver nanoparticles by *Bacillus subtilis* and their antibacterial activity. *Saudi Journal of Biological Sciences*. 27(8), 2185–2191. <https://doi.org/10.1016/j.sjbs.2020.04.026>
36. **Ghodake, G.S.; Deshpande, N.G.; Lee, Y.P.; Jin, E.S. (2010)** . Pear fruit extract-assisted room-temperature biosynthesis of gold nanoplates., *Colloids and Surfaces B: Biointerfaces*, 75, 584-589.
37. **Salim, A.A.; Bidin, N.; Lafi, A.S. and Huyop, F.Z. (2017)**. Antibacterial activity of PLAL synthesized nanocinnamon. *Materials & Design*. 132(1), 486–495. <https://doi.org/10.1016/j.matdes.2017.07.014>
38. **Kalpana, V. N. & Devi Rajeswari, V. (2018)**. A review on green synthesis, biomedical applications, and toxicity studies of ZnO NPs. *Bioinorganic chemistry and applications*, 2018.
39. **Ulrike, A.; Fischer, Reinhold Carle, Dietmar ,R.; Kammerer (2011)** Identification and quantification of phenolic compounds from pomegranate (*Punica granatum* L.) peel, mesocarp, aril and differently produced juices by HPLC-DAD–ESI/MSn, *Food Chem*. 127 (2) (2011) 807–821
40. Beatriz, R. Sumere, et al., (2018). Combining pressurized liquids with ultrasound to improve the extraction of phenolic compounds from pomegranate peel (*Punica granatum* L.), *Ultrason Sonochem*. 48, 151-162.
41. Vedashree, M. Asha, M. R., Roopavati, C. and Naidu, M. M. (2020). Characterization of volatile components from ginger plant at maturity and its value addition to ice cream. *Journal of food science and technology*, 57(9), 3371–3380..
42. Wannes, A. W. , Mhamdi, B. , Sriti, J. , Ben Jemia ,M., Ouchikh ,O. , Hamdaoui, G Kchouk, M. E. and Marzouk, B. (2010) Antioxidant activities of the essential oils and methanol extracts from myrtle (*Myrtus communis* var. *italica* L.) leaf, stem and flower. *Food Chem Toxicol*. 48(5):1362-70.
43. **Abdeen,S. ; Geo,S.; Sukanya.P. (2014)**.Nano Dimens. Int . J.(5):pp.155-162.
44. **Adu-Gyamfi, A.; Torgby-Tetteh, W. and Appiah, V. (2012)**. Microbiological Quality of Chicken Sold in Accra and Determination of D10-Value of *E. coli*. *Food and Nutrition Sciences*,(3) 693-698.
45. Alfekaik, D. F., & AL-Hilfi, S. A. (2016). Fatty acids composition by (GC-MS) and most important physical chemicals parameters of seed oil pomegranate and grape seeds. *Journal of Biology, Agriculture and Healthcare*, 6(8), 25-32.

46. **Facciola, S. Cornucopia:** a Source Book of Edible Plants. Kampong Publications, Vista, California. (1990) 166.
47. Abd Ali, M. A., & Shareef, A. A. (2021). Green Synthesis of Silver Nanoparticles by *Enterobacter Aerogenes* Bacteria in Combination with Antibiotics Against Multidrug Resistance *Streptococcus Mitis* Isolated from Oral Cavity of Some Dental Caries Patients in Misan City. *Annals of the Romanian Society for Cell Biology*, 13768-13789.
48. **Alwan, S. H., & Al-Saeed, M. H. (2021).** Biosynthesized silver nanoparticles (using *Cinnamomum zeylanicum* bark extract) improve the fertility status of rats with polycystic ovarian syndrome. *Biocatalysis and Agricultural Biotechnology*, 38, 102217.
49. **Sankar, R.; Karthik, A.; Prabu, A.; Karthik, S.; Shivashangari, K.S.; Ravikumar, V. (2013).** *Origanum vulgare* mediated biosynthesis of silver nanoparticles for its antibacterial and anticancer activity. *Colloids Surf. B Biointerfaces* 108, 80–84. <https://doi.org/10.1016/j.colsurfb.2013.02.033>.